# A Switchable Matching Circuit for Compact Wideband Antenna Designs

Yue Li, Zhijun Zhang, *Senior Member, IEEE*, Wenhua Chen, *Member, IEEE*, Zhenghe Feng, *Senior Member, IEEE*, and Magdy F. Iskander, *Fellow, IEEE*

***Abstract*—A novel compact wideband antenna, which adopts a multi-state switchable matching circuit, is proposed in this paper. The design of the switchable matching is systematically studied and a two-step iterative procedure is used to obtain optimized values for both the bandwidth division between the various stages and the matching circuit components in each stage. Without loss of generality, a meander line monopole, with dimensions of $80 \times 10 \times 10$ $\mathrm{mm}^3$, is used as the radiator in the proposed wideband antenna design. To validate the proposed new design, a four-state matching circuit controlled by four PIN diodes is fabricated and measured. The reflection coefficient of the prototype antenna is found to be better than $-7.3$ dB, and the peak gain is higher than $-3$ dBi across the 470–770 MHz bandwidth for the Integrated Services Digital Broadcasting-Terrestrial (ISDB-T) application.**

***Index Terms*—Iterative gradient searching, PIN diode, switchable matching circuits, wideband matching.**

## I. Introduction

With the rapid development of wireless communication systems, there is a significant interest in providing more digital broadcasting services to small mobile handsets. For example, Integrated Services Digital Broadcasting-Terrestrial (ISDB-T) can deliver television programs or other multimedia content directly to mobile terminals. ISDB-T operates at the frequency range of 470–770 MHz, covering a relatively wide bandwidth of 48.4%. It is always a challenge to install a passive internal antenna in a mobile handset to cover the entire ISDB-T band. This is because the typical dimensions of a mobile handset are quite small in comparison to a quarter of the wavelength which is the antenna dimension needed to effectively transmit in the 470–770 MHz frequency band. Several promising antenna designs have been published in recent papers including the planer meander sleeve monopole antenna utilized as the radiating element in a mobile handset [1] and the conical monopole loaded with a circular patch on top studied by Zhou, *et al.* in [2]. These designs, however, occupy unacceptably large space, and, hence, some other techniques need to be investigated to design compact wideband antennas for the ISDB-T applications.

Frequency reconfigurable antenna approach represents an alternative method for designing wideband antennas [3]–[8]. This approach has the capacity of switching the operating frequency while maintaining similar radiation pattern and gain throughout the required bands. Examples of these designs include the one described in a study by Kathleen *et al.* [3], using a varactor to tune the frequency of PIFA. Similar idea is studied by Milosavljevic *et al.* [4], wherein a varactor is loaded at the end of a PIFA antenna and the operating frequency was tuned by varying the capacitance. This reconfigurable method is also used in another study [5], where a varactor is loaded in a slot antenna at a fixed location to achieve a wide tunability range of the first resonant frequency ($\mathrm{f}_1$) and the second resonant frequency ($\mathrm{f}_2$) and a frequency ratio ($\mathrm{f}_2/\mathrm{f}_1$) that ranges from 1.2 to 1.65. If different varactor locations are chosen, a wider frequency ratio could be achieved with a range of 1.3 to 2.67 [6]. PIN diodes are also used to change the length of antenna elements [7], adjust locations of feed points [8], and help tune the antennas and achieve impedance matching. Some of these antenna designs actually covered multiple bands including the GSM850 (824–894 MHz), GSM900 (880–960 MHz), DCS (1710–1880 MHz), PCS (1850–1990 MHz), and UMTS (1920–2170 MHz) bands [8].

The circuit used for impedance matching can also be reconfigurable. The antenna impedance can be matched in a relatively wide bandwidth by several states in a switchable matching circuit. The matching circuit designed by Mingo, *et al.* [9] can generate a great number of impedance values uniformly distributed on the Smith Chart. In this case, the circuit is composed of several lumped capacitances controlled by several PIN diodes. In a switchable matching circuit, several matching components are needed and lumped components are usually more preferred than distributed ones as they provide advantages, such as small footprint, ease of switching, and wide-working frequency range. The insertion losses of lumped components, however, cannot be ignored, but they are often considered acceptable in antennas designed for mobile communication applications.

In this paper, a compact wideband monopole antenna with a switchable matching circuit is proposed. In a study by Kang *et al.* [10], a preliminary switchable matching circuit was proposed, and some preliminary simulations were presented. In

Manuscript received July 08, 2009; revised December 24, 2009; accepted April 18, 2010. Date of publication September 02, 2010; date of current version November 03, 2010. This work was supported in part by the National Basic Research Program of China under Contract 2009CB320205, in part by the National High Technology Research and Development Program of China (863 Program) under Contract 2007AA01Z284, in part by the National Natural Science Foundation of China under Contract 60771009, and in part by the National Science and Technology Major Project of the Ministry of Science and Technology of China 2009ZX03006-008.

Y. Li, Z. Zhang, W. Chen, and Z. Feng are with State Key Laboratory on Microwave and Digital Communications, Tsinghua National Laboratory for Information Science and Technology, Department of Electronic Engineering, Tsinghua University, Beijing 100084, China (e-mail: zjzh@tsinghua.edu.cn).

M. F. Iskander is with HCAC, University of Hawaii at Manoa, Honolulu, HI 96822 USA (e-mail: iskander@spectra.eng.hawaii.edu).

Color versions of one or more of the figures in this paper are available online at http://ieeexplore.ieee.org.

Digital Object Identifier 10.1109/TAP.2010.2071345

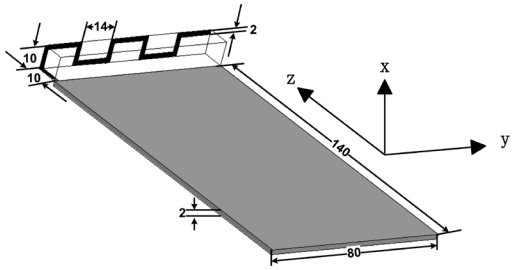


Fig. 1. 3-D geometry of proposed antenna (unit: mm).

this follow-up manuscript, a matching procedure and a switchable matching circuit topology are systematically described, and a dual-step gradient optimization method is introduced to determine the component values of a matching circuit. Specifically, a four-state switchable matching circuit is designed using four lumped components controlled by four PIN diodes, and each component is reused twice to minimize the complexity of the overall system. A prototype of meander line monopole antenna is fabricated as an example of a switchable system to validate the developed matching technique. The obtained results show that the designed antenna can cover the entire ISDB-T (470–770 MHz) band with $S_{11}$ better than $-7.3\,\mathrm{dB}$ when combining the four matching states. The gain and radiation patterns are also measured, and the obtained results are presented in the following sections.

The manuscript is arranged as follows. In Section II, the matching technique is studied and the topology of the matching circuit is described. In Section III, a gradient optimization method is introduced to determine values of the matching circuit components. The fabrication of the proposed antenna with a matching circuit is then described and the results of the measured reflection coefficient, gain, and radiation patterns are shown in Section IV. Conclusions are presented in Section V.

## II. Switchable Matching Circuit Design

### A. Compact Meander Line Monopole

Without loss of generality, a compact meander line monopole, shown in Fig. 1, is used here to demonstrate the proposed reconfigurable matching technique. The antenna dimensions are $80 \times 10 \times 10\ \mathrm{mm}^3$ ($0.125\ \lambda \times 0.016\ \lambda \times 0.016\ \lambda$). The width of strip is 2 mm. The antenna is installed at the edge of the ground plane, which is made up of a 2-mm thick $140 \times 80\ \mathrm{mm}^2$ single side FR4 board ($\varepsilon_r = 4.4$). The impedance locus of the antenna is shown in Fig. 2, and the impedance at 770 MHz and 470 MHz are marked by Markers 1 and 2, respectively. This impedance locus is a good representative of most monopole antennas. In a low frequency band, the antenna has a capacitive characteristic, while in a high frequency band, its impedance is inductive. The original reflection coefficient without matching is shown in Fig. 3, and the reflection coefficient bandwidth of $-5\,\mathrm{dB}$ is only 100 MHz.

### B. Matching Circuit Design

It is well known that for any given impedance, there is more than one matching circuit, which could be used to achieve good impedance matching [11]. In the example shown in

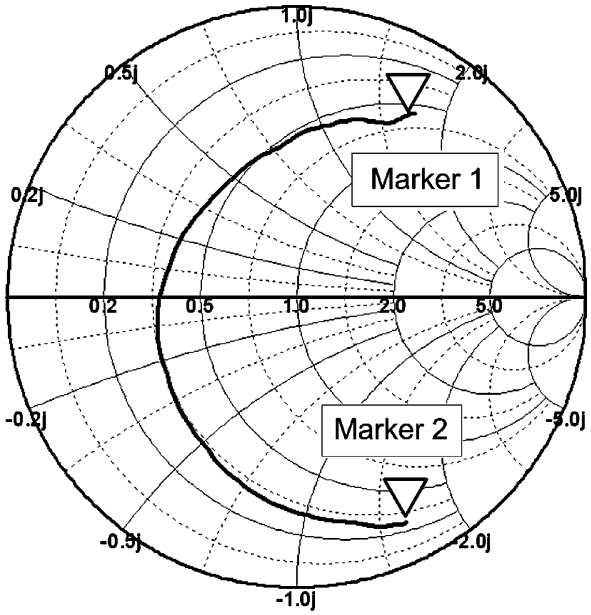


Fig. 2. Resonant antenna curve on Smith Chart (470–770 MHz).

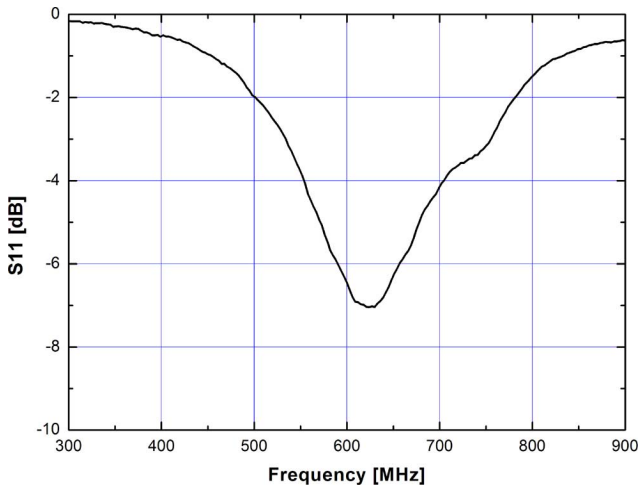


Fig. 3. Reflection coefficient of proposed antenna without matching.

Fig. 4(a) and (b), all four circuits can be used as a single frequency matching for the impedance at location X. Using the left side circuit in Fig. 4(a) as an example, the series capacitor moves the antenna impedance from location X along the large anticlockwise curve, while the shunt inductor moves the impedance along the small anticlockwise curve to the matching point. Combining the effect of both components, the impedance at location X is successfully matched to 50 Ω. In the proposed procedure, the goal of a reconfigurable matching is to match different portions of the impedance locus, which are equivalent to different frequency bands, by using different circuits. This might sound simple, but in practice the matching must be carefully designed to achieve the desired performance.

For example, if the desired frequency range of the antenna is divided into four segments, as shown in Fig. 5, with Band 1 having the lowest frequency band and Band 4 having highest frequency, the total number of possible matching circuits will

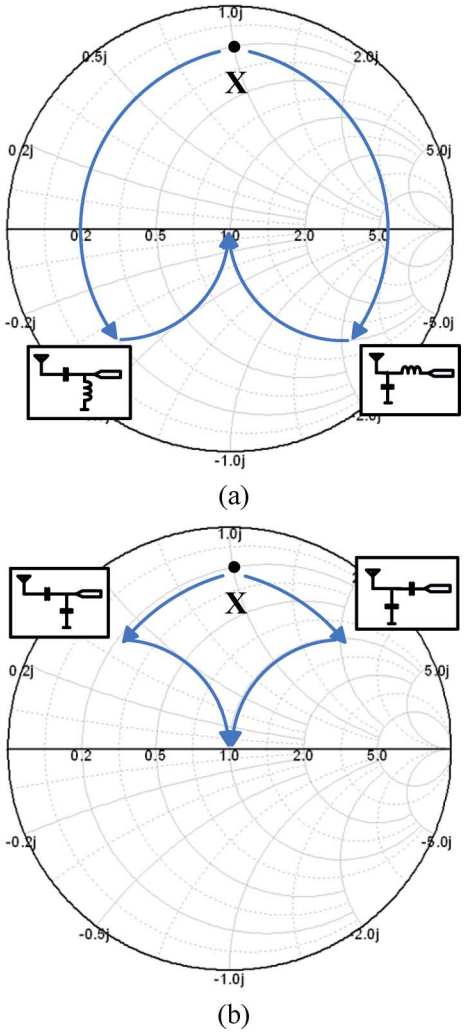


Fig. 4. Four different ways to match the impedance at location X.

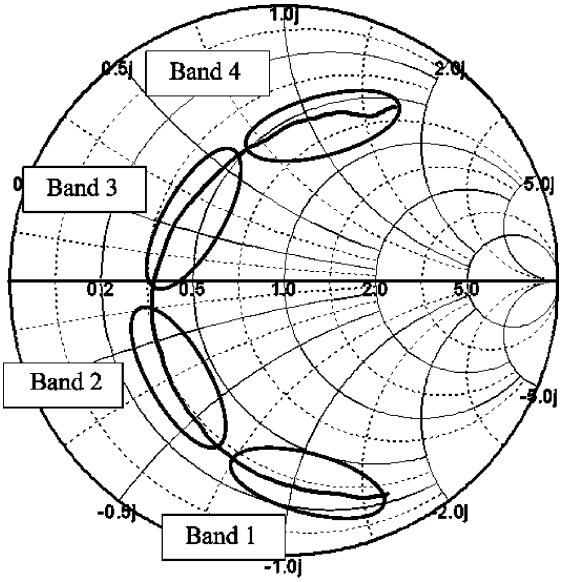


Fig. 5. Division of the whole bandwidth into four regions.

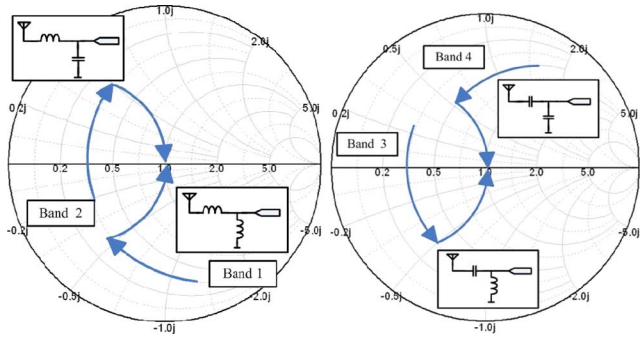


Fig. 6. Matching circuits for four bands.

be sixteen (i.e., four segments multiplied by four possible circuit elements, see Fig. 4 for each segment). In other words, one way to implement this wideband impedance matching is to utilize four independent circuits, one for each band. Assuming that each matching circuit uses two components, the matching arrangement mentioned above will require eight components and two single-pole four-throw (SP4T) switches.

Another way to obtain the required four matching states could be based on an overall and simultaneous optimization of one set of matching components. In this case, when selecting the matching components and the circuit layout, reuse becomes a primary consideration. By using one shunt and one series components, as shown in Fig. 6, it is possible to match all four bands independently. Looking from the antenna side, a series inductor and a shunt inductor can be used to match Band 1, a series inductor and a shunt capacitor for Band 2, a series capacitor and a shunt inductor for Band 3, and a capacitor and a shunt capacitor for Band 4.

In Fig. 6, although the matching circuits used to match the four regions have been chosen to have similar topologies, if there are no constraints on the matching circuit design, the result could still be eight different component values. The following shows that the circuit can be simplified by optimizing the matching circuit as a whole and while covering the required frequency rang. Here, single-pole 2-throw (SP2T) switches are used as the switchable components. Because each SP2T switch can provide two states, N switches can then provide a maximum of $2^N$ states. Two possible topologies of such matching circuits are shown in Fig. 7(a) and (b). The maximum numbers of states in these two topologies are 4 and 8, respectively.

In the circuit shown in Fig. 7(a), for example, a total of four components are used and each component is active in two states. When the Switch A is in Position 1 and Switch B is in Position 1, and then Band 1 can be matched. The other matching configurations are listed in Table I.

## III. Parameter Optimization

After deciding on the topology of the matching circuit, this section focuses on describing the procedure for selecting values of the circuit components. There are actually two related optimizations in this process. The first one is on how to divide the entire frequency band into several regions, while the other is on the determination of the values of the components. As may be expected, when the frequency span of a region gets narrower, it is easier to achieve good matching in this region. This, how-

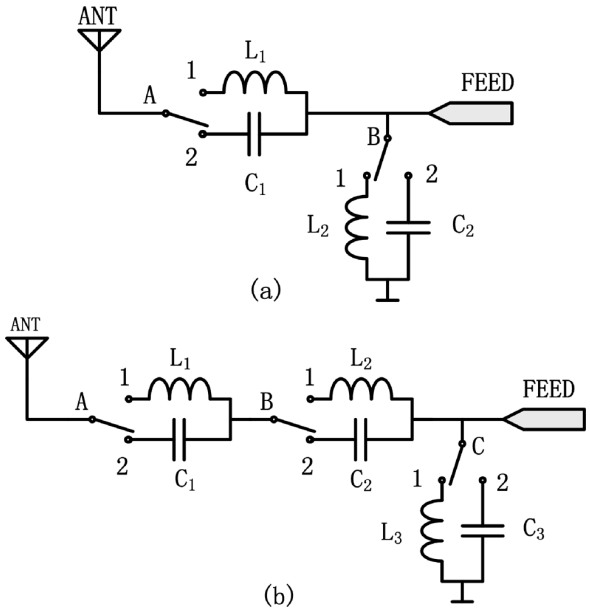


Fig. 7. Switchable matching circuit (a) 2 SP2T, 4 states and (b) 3 SP2T, 8 states.

TABLE I
MATCHING CONFIGURATION OF SWITCH A AND B

| Switch A | Switch B | Matching Region | $Z_m(f)$ |
|---|---|---|---|
| 1 | 1 | Band 1 | $Z_1(f)$ |
| 1 | 2 | Band 2 | $Z_2(f)$ |
| 2 | 1 | Band 3 | $Z_3(f)$ |
| 2 | 2 | Band 4 | $Z_4(f)$ |

ever, makes it more difficult to achieve matching over the entire band, since the process results in a set of well-matched but narrow bands. Naturally, an optimization procedure of multiple iterations is required to achieve an optimized matching over the entire band.

As an example, in the circuit shown in Fig. 7(a), all matching components and switches are considered as ideal ones. As a result, the component value vector $\mathbf{c}$ and frequency band edge vector $\mathbf{f}$ can be expressed by (1)

$$\mathbf{c} = [\,L_1 \quad C_1 \quad L_2 \quad C_2\,],\ \mathbf{f} = [\,f_1 \quad f_2 \quad f_3 \quad f_4 \quad f_5\,]. \tag{1}$$

In vector $\mathbf{f}$, $f_1$ and $f_5$ are the band edges of the overall band, with $f_1 = 470$ MHz and $f_5 = 770$ MHz. In addition, $f_2$, $f_3$, and $f_4$ are sub-band edges, which segment the overall band. The vectors $\mathbf{c}$ and $\mathbf{f}$ are variables that need to be optimized. The cost function $Err$ is given in Formulas (2)–(4). $Z_{ant}(f)$ is the measured input impedance without matching. $Z_m(f)$ is the matched input impedance in each band, as listed in Table I. $RL_m$ is the optimization goal of return loss in the $m_{th}$ sub-band. In this example, $RL_m$ is set to 10 dB for all four sub-bands. The $Err$ is the sum of error of all four sub-bands. In each sub-band, the error is calculated by integrating the positive difference between the antenna response and the goal over the specific sub-band. If at one frequency the antenna response is better than the goal, the error value at that frequency is 0, which means it doesn't contribute to the overall cost function

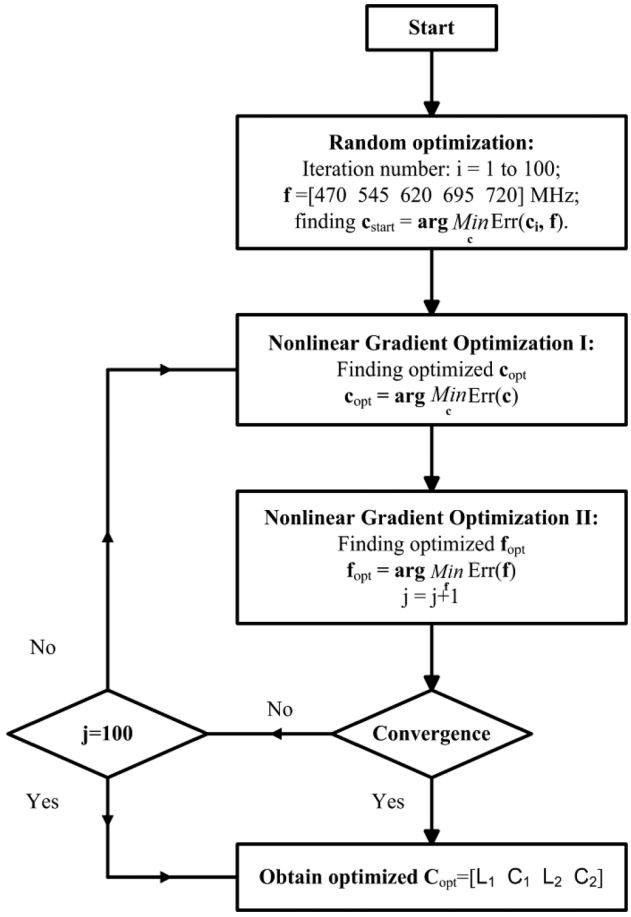


Fig. 8. Flow chart for optimization.

$$Err = \sum_{m=1}^{4} Err_m \tag{2}$$

$$Err_m = \sum_{f_m}^{f_{m+1}} \max\left(20\log\left(\frac{Z_m(f)-Z_c}{Z_m(f)+Z_c}\right) + RL_m, 0\right)$$

$$f_m \le f \le f_{m+1} \tag{3}$$

$$Z_1(f) = \frac{(Z_{ant}(f) + j2\pi fL_1)\cdot j2\pi fL_2}{Z_{ant}(f) + j2\pi fL_1 + j2\pi fL_2} \quad f_1 \le f \le f_2$$

$$Z_2(f) = \frac{Z_{ant}(f) + j2\pi fL_1}{1 + (Z_{ant}(f) + j2\pi fL_1)\cdot j2\pi fC_2} \quad f_2 \le f \le f_3$$

$$Z_3(f) = \frac{(1 + j2\pi fC_1\cdot Z_{ant}(f))\cdot j2\pi fL_2}{1 + j2\pi fC_1\cdot Z_{ant}(f) + j2\pi fL_2\cdot j2\pi fC_1}$$

$$f_3 \le f \le f_4$$

$$Z_4(f) = \frac{1 + j2\pi fC_1\cdot Z_{ant}(f)}{j2\pi fC_1 + j2\pi fC_2 + j2\pi fC_1\cdot j2\pi fC_2\cdot Z_{ant}(f)}$$

$$f_4 \le f \le f_5. \tag{4}$$

The optimization procedure is illustrated in Fig. 8. It includes the following steps:

1) Random optimization: 100 values of vector $\mathbf{c_i}$ are selected randomly between 0 and 30 (nH/pF), as candidates for starting values. Even distribution is selected as the value of

TABLE II
OPTIMIZED VALUE

| Component | $L_1$ (nH) | $L_2$ (nH) | $C_1$ (pF) | $C_2$ (pF) |
|---|---|---|---|---|
| Optimized value | 10.3 | 15.6 | 4.7 | 4.6 |

$\mathbf{f}$, i.e., $f_2 = 545$ MHz, $f_3 = 620$ MHz, and $f_4 = 695$ MHz. $Err(\mathbf{c_i}, \mathbf{f})$ is calculated to find the $\mathbf{c_{start}}$, whose $Err$ is the minimum.

2) Nonlinear gradient optimization I: The optimized $\mathbf{c_{opt}}$ is found when $\mathbf{f}$ is fixed; that is, the optimized values of $L_1$, $L_2$, $C_1$, and $C_2$ for the fixed four sub-frequency bands are found. The object function and constraints are illustrated in Formula (5). The index j is utilized as the counter of optimization times while setting $j = 0$ first

$$\begin{aligned} obj: &\quad \min\ Err(\mathbf{c}) \\ s.t.: & \\ & 0 \le L_1 \le 30\ \text{nH} \\ & 0 \le C_1 \le 30\ \text{pF} \\ & 0 \le L_2 \le 30\ \text{nH} \\ & 0 \le C_2 \le 30\ \text{pF}. \end{aligned} \tag{5}$$

3) Nonlinear gradient optimization II: The optimized $\mathbf{f_{opt}}$ is found when $\mathbf{c}$ is fixed; that is, the optimized ranges of sub-frequency bands for four matching circuits are found. The object function and constraints are illustrated as follows:

$$\begin{aligned} obj: &\quad \min\ Err(\mathbf{f}) \\ s.t.: &\quad f_1 < f_2 < f_3 < f_4 < f_5. \end{aligned} \tag{6}$$

4) If the calculated error converges, the optimized $\mathbf{c_{opt}}$ is obtained. Otherwise, Step 3 is repeated. The index j then increases by one.
5) The process of optimization terminates when it converges or $j = 100$. The latest $\mathbf{c}$ is chosen as the optimized $\mathbf{c_{opt}}$.

The method to find the value of $\mathbf{c_{start}}$ in Step 1 is based on random optimization. The optimization goal in Step 2 and 3 is to find the minimum of constrained nonlinear multivariable function based on the iterative gradient searching. The optimization procedure has been run several times and converges with iterations less than 100. As a result, $j = 100$ is set to guarantee the final convergence. The final results are not sensitive to the starting values. Various initial values, which are randomly distributed between 0 and 30 (nH/pF), are trialed to test the robustness of the optimization procedure and it always converged to the same values.

The optimization values of the four components are listed in Table II. The goal of the optimization without any parasitic parameters and insertion loss is to prove the design strategy and find initial values for practical tuning.

## IV. ANTENNA FABRICATION AND MEASUREMENT RESULTS

To demonstrate the validity of the presented matching strategy, a meander line antenna was fabricated and matched. The fabrication of a meander line monopole antenna, which is fed by a 50 Ω coaxial cable, is shown in Fig. 9. The antenna

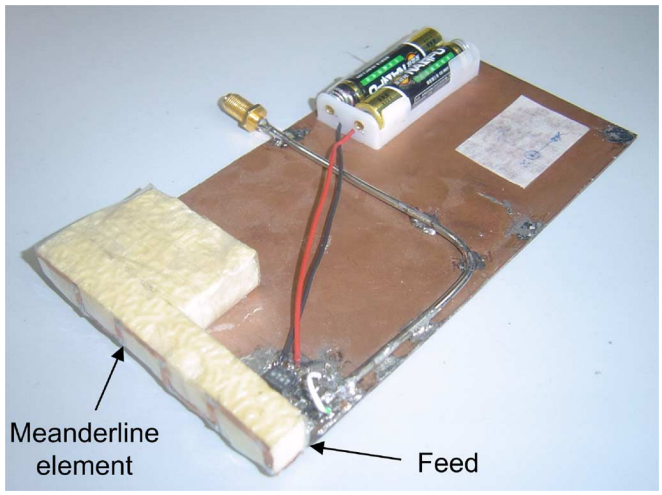


Fig. 9. Fabrication of proposed antenna.

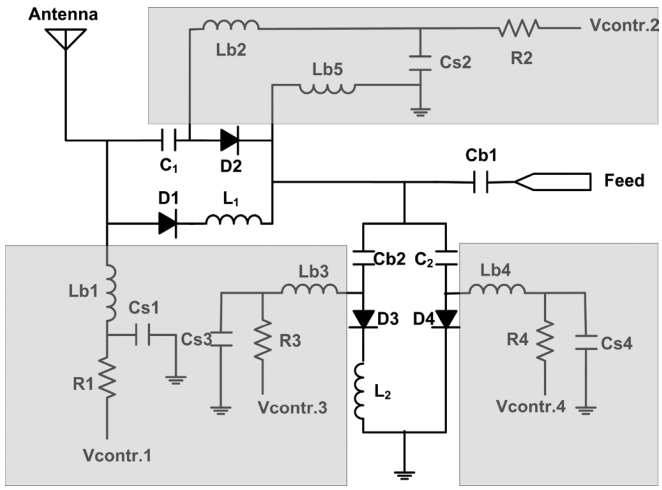


Fig. 10. Schematic diagram of switchable matching circuit.

TABLE III
MATCHING CONFIGURATION OF D1-D4

| Matching Region | D1 | D2 | D3 | D4 |
|---|---|---|---|---|
| Band 1 | ON | OFF | ON | OFF |
| Band 2 | ON | OFF | OFF | ON |
| Band 3 | OFF | ON | ON | OFF |
| Band 4 | OFF | ON | OFF | ON |

is made of a flat metallic strip, meandered and attached to the outer side of a foam support, with dimensions of $80 \times 10 \times 10$ $\text{mm}^3$. The 3 V control voltage for the switch is supplied using two AA batteries.

The schematic diagram of the four-states of a switchable matching circuit is shown in Fig. 10. The gray area in Fig. 10 is the bias circuit and the clear area is the primary signal path. Four PIN diodes (Philips BAP64-03) are used to control $L_1$, $L_2$, $C_1$, and $C_2$. The configuration of the four PIN diodes for different matching states is shown in Table III. The bias resistances (R1-R4) are all 46 Ω, and the inductance (Lb1-

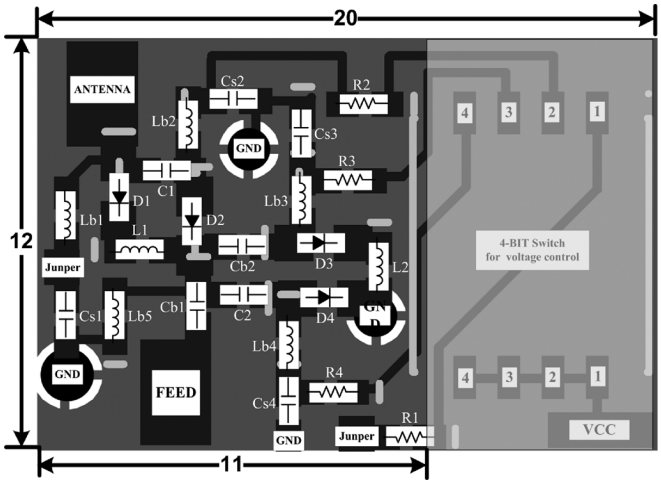


Fig. 11. Dimension of switchable matching circuit PCB (unit: mm).

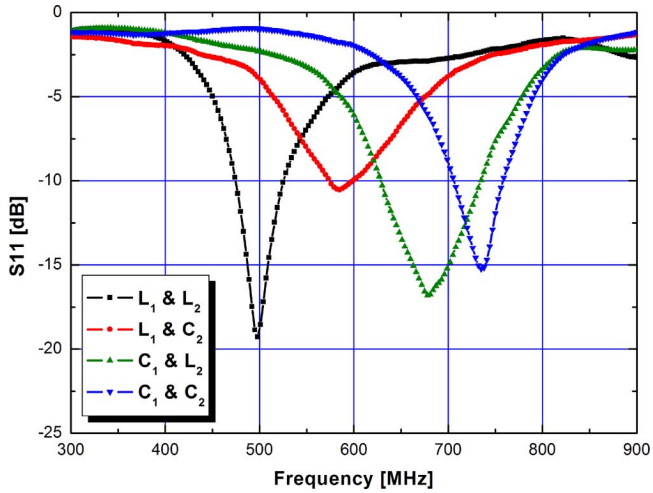


Fig. 12. Reflection coefficient with matching circuit.

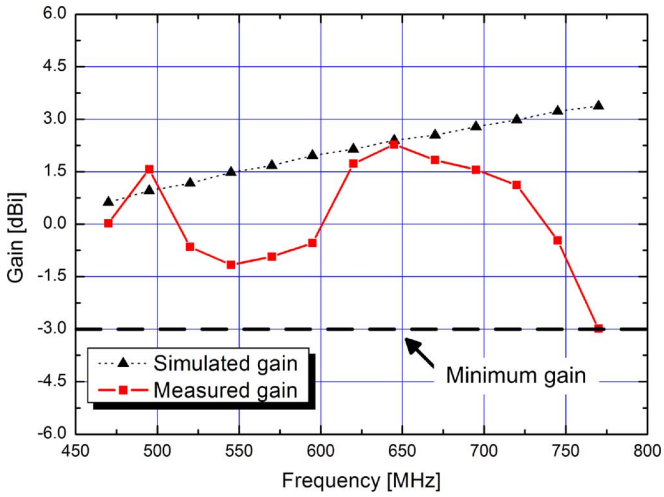


Fig. 13. Measured and simulated gain.

Lb5) chokes RF signal from the matching circuit to control the voltage source with a value of 120 nH. RF signal shorting capacitances (Cs1-Cs4) are all 470 pF, and the DC block capacitance (Cb1 and Cb2) are 100 pF each. The entire matching network with voltage bias circuit was printed on a 1-mm thick $11 \times 12$ mm$^2$ PCB, as shown in Fig. 11. If the antenna is to serve as a transmitting antenna, the power handling capability must be considered when designing the matching circuit. To transmit a 30 dBm signal, a bias voltage of 10 V or more is required. However, the antenna proposed in this paper is supposed to be used as a receiving antenna, so a 3 V bias voltage can already guarantee the positive bias status.

The values of key components $L_1$, $L_2$, $C_1$, and $C_2$ are different from the optimized set-up due to the parasitic parameters introduced by the components and routing from the PCB. Also, the insertion loss of PIN diodes must be involved. Starting from the simulated values of the four components, some iterative tuning procedure must be involved based on the frequency response. The optimizing method is almost identical to the one used in the simulation. Unlike continuous value used in simulation, discrete components with parasitic effect are replaced at each iteration step. The series components $L_1$ and $C_1$ affect the center frequency for four bands, while shunt components $L_2$ and $C_2$ decide the return loss. As a result, a tradeoff between center frequency and return loss in each band must be considered in the components values tuning. The final values of $L_1$, $L_2$, $C_1$, and $C_2$ soldered on the PCB are 12 nH, 18 nH, 4.7 pF, and 2.2 pF.

The measured reflection coefficient of the proposed antenna with the matching circuit is shown in Fig. 12. As seen in the figure, the combined bandwidth covers the whole required ISDB-T frequency band of 470–770 MHz with $S_{11}$ better than $-7.3$ dB.

Simulated gain and measured gain in the desired bands are shown in Fig. 13. The measured gain peaks at 2.9 dBi and is better than $-3$ dBi, which is the minimum gain limit required by the system specification across the whole band. The difference between the straight line and the dashed line is attributed to the insertion loss introduced by the matching components. The average insertion loss is around 2 dB in the ISDB-T band. The insertion loss is mainly introduced by non-ideal lumped components and PIN diodes. And it can be reduced by adopting high quality components and low insertion loss switches in the matching network. There is a discrepancy at the 495 MHz frequency shown in Fig. 13, where the measured gain is higher than the ideal one. This is due to the error introduced by the chamber measurement. Furthermore, at the low end of the measured frequency range, the chamber uncertainty can be up to 2 dB. It can be observed that the antenna has a below average gain when the shunt matching component is switched to the capacitor, which corresponds to bands of 545–590 MHz and 725–770 MHz. Further investigation and improvement on this phenomenon are needed if better performance is required.

The radiation patterns at 495 and 720 MHz are shown in Figs. 14 and 15, respectively. A quasi-omnidirectional pattern is achieved in the x-y plane.

## V. Conclusion

In this paper, a compact frequency reconfigurable monopole antenna with switchable matching circuit is presented. The monopole antenna matching method has been systematically

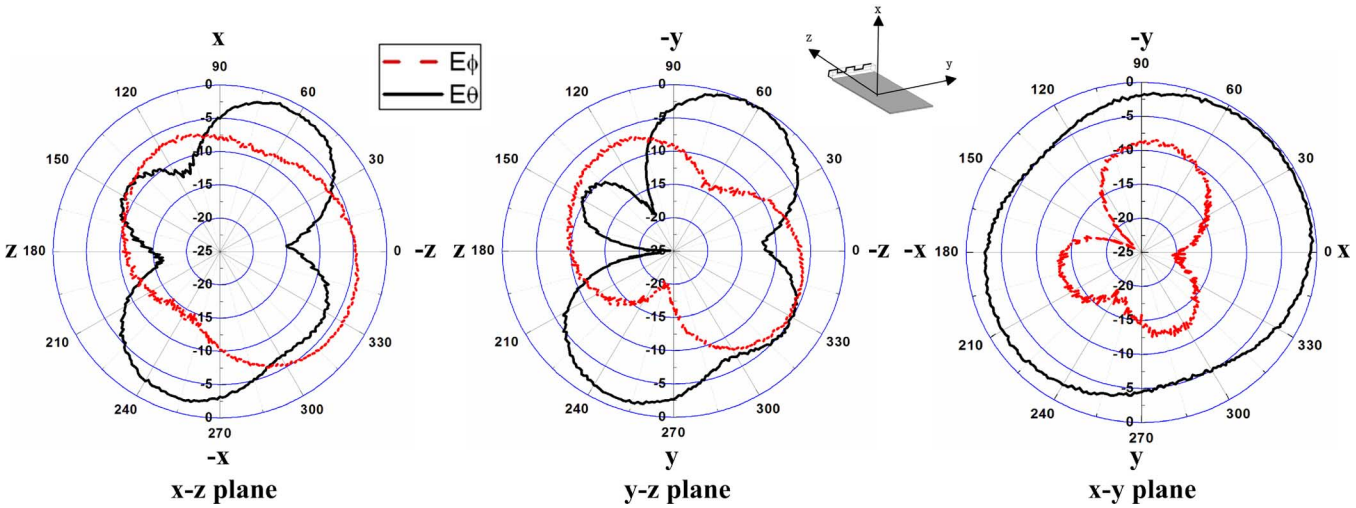


Fig. 14. Radiation pattern at 495 MHz.

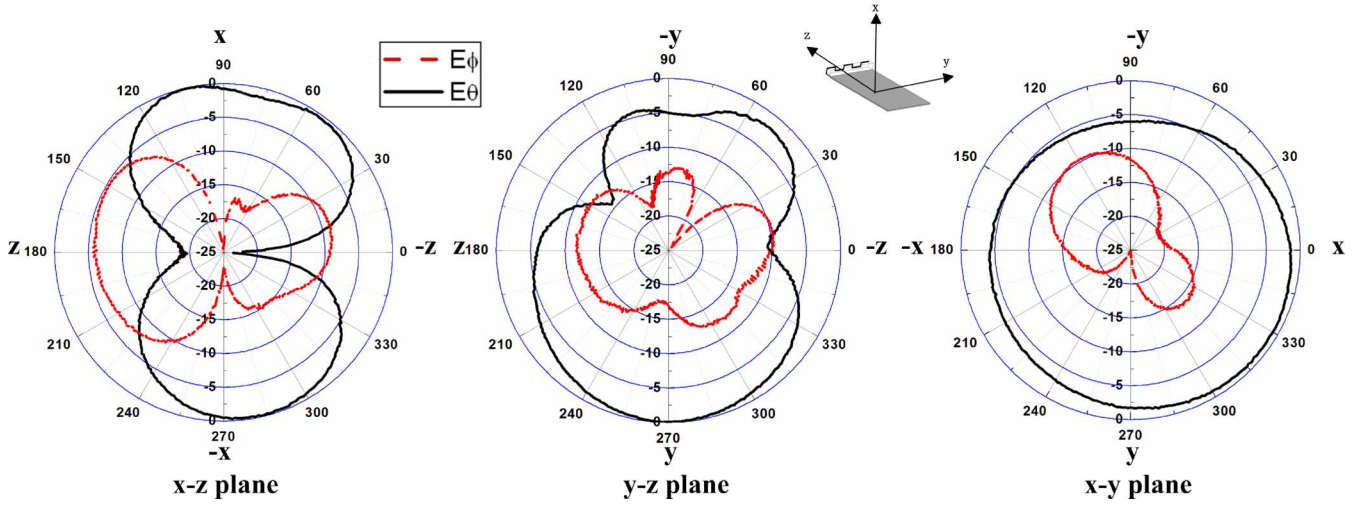


Fig. 15. Radiation pattern at 720 MHz.

studied and optimized. An iterative gradient optimization method is introduced to divide the band of interest into suitable regions and to determine the four optimized component values that would achieve matching over the entire band. A meander line monopole antenna and a four-state matching circuit are fabricated and measured to validate the proposed technique. Simulation and experimental results show that the antenna can cover the entire ISDB-T (470–770 MHz) frequency band with $S_{11}$ better than $-7.3$ dB. The gain and radiation patterns of the proposed antenna are also measured. The proposed matching technique can, therefore, successfully be utilized for other applications using different antennas over different frequency bands.

## REFERENCES

[1] B. H. Sun, J. F. Li, T. Zhou, and Q. Z. Liu, "Planar meander sleeve monopole antenna for DVB-H/GSM mobile handsets," *Electron. Lett.*, vol. 44, no. 8, pp. 508–509, Apr. 2008.

[2] S.-G. Zhou, B.-H. Sun, Y.-F. Wei, and Q.-Z. Liu, "Low profile wideband antenna with shaped beams for indoor DVB-H applications," *Electron. Lett.*, vol. 45, no. 23, pp. 1151–1152, Nov. 2009.

[3] K. L. Virga and Y. Rahmat-Samii, "Low-profile enhanced-bandwidth PIFA antennas for wireless communications packaging," *IEEE Trans. Microwave Theory Tech.*, vol. 45, pp. 1879–1888, Oct. 1997.

[4] Z. D. Milosavljevic, "A varactor tuned DVB-H antenna," in *Proc. Int. Conf. on Antenna Technology Small Antennas and Novel Metamaterials*, Cambridge, U.K., 2007, pp. 124–127.

[5] N. Behdad and K. Sarabandi, "A varactor-tuned dual-band slot antenna," *IEEE Trans. Antennas Propag.*, vol. 54, pp. 401–408, Feb. 2006.

[6] N. Behdad and K. Sarabandi, "Dual-band reconfigurable antenna with a very wide tunability range," *IEEE Trans. Antennas Propag.*, vol. 54, pp. 409–416, Feb. 2006.

[7] D. Peroulis, K. Sarabandi, and L. P. B. Katehi, "Design of reconfigurable slot antennas," *IEEE Trans. Antennas Propag.*, vol. 53, pp. 645–654, Feb. 2005.

[8] A. C. K. Mak, C. R. Rowell, R. D. Murch, and C.-L. Mak, "Reconfigurable multiband antenna designs for wireless communication devices," *IEEE Trans. Antennas Propag.*, vol. 55, pp. 1919–1928, Jul. 2007.

[9] J. Mingo, A. Valdovinos, A. Crespo, D. Navarro, and P. Garcia, "An RF electronically controlled impedance tuning network design and its application to an antenna input impedance automatic matching system," *IEEE Trans. Microw. Theory Tech.*, vol. 52, no. 2, pp. 489–497, Feb. 2004.

[10] Y. Kang, H. Mi, Z. Zhang, W. Chen, and Z. Feng, "A reconfigurable compact antenna for DVBH application," in *Proc. Int. Conf. on Microwave and Millimeter Wave Technology*, Apr. 2008, pp. 1882–1885.

[11] D. M. Pozar, *Microwave Engineering*, 3rd ed. New York: Wiley, 2005, ch. 5.

**Yue Li** was born in Shenyang, China, in 1984. He received the B.S. degree in telecommunication engineering from the Zhejiang University, Zhejiang, China, in 2007. He is currently working toward the Ph.D. degree at Tsinghua University, Beijing, China.

His current research interests include antenna design and theory, particularly in reconfigurable antennas, electrically small antennas and antenna in package.

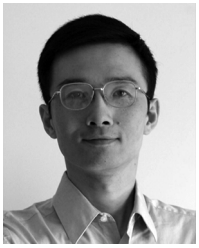

**Zhijun Zhang** (M'00–SM'04) received the B.S. and M.S. degrees from the University of Electronic Science and Technology of China (UESTC), Chengdu, in 1992 and 1995, respectively, and the Ph.D. degree from Tsinghua University, Beijing, China, in 1999.

In 1999, he was a Postdoctoral Fellow with the Department of Electrical Engineering, University of Utah, Salt Lake City, where he was appointed a Research Assistant Professor in 2001. In May 2002, he was an Assistant Researcher with the University of Hawaii at Manoa, Honolulu. In November 2002, he joined Amphenol T&M Antennas, Vernon Hills, IL, as a Senior Staff Antenna Development Engineer and was then promoted to the position of Antenna Engineer Manager. In 2004, he joined Nokia Inc., San Diego, CA, as a Senior Antenna Design Engineer. In 2006, he joined Apple Inc., Cupertino, CA, as a Senior Antenna Design Engineer and was then promoted to the position of Principal Antenna Engineer. Since August 2007, he has been with the Department of Electronic Engineering, Tsinghua University, Beijing, China, where he is a Professor.

**Wenhua Chen** (M'07) received the B.S. degree from the University of Electronic Science and Technology of China (UESTC), Chengdu, in 2001, and the Ph.D. degree from Tsinghua University, Beijing, China, in 2006.

He is currently an Assistant Professor with the State Key Laboratory on Microwave and Digital Communications, Tsinghua University. His research interests include computational electromagnetics, reconfigurable and smart antennas, and high-efficiency power amplifiers. He has authored and coauthored over 30 journal and conference papers.

**Zhenghe Feng** (SM'92) received the B.S. degree in radio and electronics from Tsinghua University, Beijing, China, in 1970.

Since 1970, he has been with Tsinghua University, as an Assistant, Lecturer, Associate Professor, and Full Professor. His main research areas include numerical techniques and computational electromagnetics, RF and microwave circuits and antenna, wireless communications, smart antenna, and spatial temporal signal processing.

**Magdy F. Iskander** (F'93) is the Director of the Hawaii Center for Advanced Communications (HCAC), College of Engineering, University of Hawaii at Manoa, in Honolulu (http://hcac.hawaii.edu). He is also a Co-Director of the NSF Industry/University joint Cooperative Research Center between the University of Hawaii, University of Arizona, Arizona State University, and the RPI and the Ohio State University. He was a Professor of Electrical Engineering and the Engineering Clinic Endowed Chair Professor at the University of Utah, Salt Lake City, for 25 years. He was also the Director of the Center of Excellence for Multimedia Education and Technology. In 1986, he established the Engineering Clinic Program at the University of Utah to attract industrial support for projects for undergraduate engineering students and was the Director of this program until joining the University of Hawaii in 2002. From 1997–99 he was a Program Director, in the Electrical and Communication Systems Division at the National Science Foundation. He spent sabbaticals and other short leaves at Polytechnic University of New York; Ecole Superieure D'Electricite, France; UCLA; Harvey Mudd College; Tokyo Institute of Technology; Polytechnic University of Catalunya, Spain; University of Nice-Sophia Antipolis, and at several universities in China including Tsinghua University. He authored a textbook on *Electromagnetic Fields and Waves* (Prentice Hall, 1992; and Waveland Press, 2001) edited the *CAEME Software Books*, Vol. I, 1991, and Vol. II, 1994; and edited four other books on *Microwave Processing of Materials*, all published by the Materials Research Society, 1990–1996. He edited the 1995 and 1996 *International Conference on Simulation and Multimedia in Engineering Education Proceedings*. He has published over 200 papers in technical journals, has eight patents, and has made numerous presentations in technical conferences. He is the Founding Editor of the journal, *Computer Applications in Engineering Education* (Wiley). This journal is now in its 18th year, and received the Excellence in Publishing Award, by the Association of the American Publishers, in 1993. His ongoing research contracts include propagation models, low-cost phased array antenna designs, IED and UXO targets detection and classification, HF radar for homeland security applications, and several other research projects sponsored by corporate sponsors including Raytheon, Trex, Motorola, Kyocera Wireless, Corning, Inc., BAE Systems, and L-3 Communications.

Dr. Iskander is a Fellow of the IEEE and was a member of the National Research Council Committee on Microwave Processing of Materials. He received the 1985 Curtis W. McGraw ASEE National Research Award, 1991 ASEE George Westinghouse National Education Award, 1992 Richard R. Stoddard Award from the IEEE EMC Society, the 2000 University of Utah Distinguished Teaching Award, and the 2002 Kuhina (Ambassador) Award from the Hawaii Visitors and Convention Bureau. He was a Guest Editor of a Special Issue on Wireless Communications Technology for the IEEE TRANSACTIONS ON ANTENNAS AND PROPAGATION in May 2002, Co-Guest Editor of a Special Issue of the *IEICE Journal* in Japan (September 2004), and a Co-Guest Editor of a Special Issue on Wireless Communications for the IEEE TRANSACTIONS ON ANTENNAS AND PROPAGATION in 2006. He is the 2002 President of the IEEE Antennas and Propagation Society, Vice President in 2001, and was a member of the IEEE APS AdCom from 1997 to 1999. He was the General Chair of the 2000 IEEE AP-S Symposium and URSI meeting in Salt Lake City, UT, the General Chair of the IEEE Conference on Wireless Communications Technology, in 2003, in Hawaii, the General Chair of the 2005 IEEE/ACES joint conference on Wireless Communications and Applied Computational Electromagnetics, and the General Chair for the 2007 IEEE Antennas and Propagation International Symposium in Honolulu, HI. He was also a Distinguished Lecturer for the IEEE AP-S (1994–97).